BioScientific Review (BSR)
Volume 8 Issue 2, 2026
ISSN$_{(P)}$: 2663-4198, ISSN$_{(E)}$: 2663-4201
Homepage: https://journals.umt.edu.pk/index.php/bsr

Title:	***In Silico* Repurposing of Fluoxetine: Targeting the MvfR Protein of *Pseudomonas aeruginosa***
Author (s):	Affhan Shoaib and Mumtaz Zarkhaiz
Affiliation (s):	Salim Habib University, Karachi, Pakistan
DOI:	https://doi.org/10.32350/bsr.82.04
History:	Received: October 25, 2025, Revised: February 13, 2026, Accepted: April 02, 2026, Published: April 27, 2026
Citation:	Shoaib A, Zarkhaiz M. In Silico repurposing of fluoxetine: targeting the MvfR protein of pseudomonas aeruginosa. *BioSci Rev.* 2026;8(2):45-65. https://doi.org/10.32350/bsr.82.04
Copyright:	© The Authors
Licensing:	This article is open access and is distributed under the terms of Creative Commons Attribution 4.0 International License
Conflict of Interest:	Author(s) declared no conflict of interest

A publication of
The Department of Life Sciences, School of Science
University of Management and Technology, Lahore, Pakistan

In Silico Repurposing of Fluoxetine: Targeting the MvfR Protein of *Pseudomonas aeruginosa*

Affhan Shoaib and Mumtaz Zarkhaiz*

Department of Biosciences, Salim Habib University, Karachi, Pakistan

ABSTRACT

Fluoxetine is mainly used as a selective serotonin reuptake inhibitor. However, studies have shown that it may also have antimicrobial properties and antivirulence effects. This study utilized an *in silico* repurposing and drug repositioning methodology on fluoxetine (an antidepressant drug) against *Pseudomonas aeruginosa* infection. The goal was to focus on a protein called MvfR/PqsR. This MvfR/PqsR protein is important, for controlling how bad a germ is and how it forms a group of germs that stick together. To find some compounds that can work with this MvfR/PqsR protein we used computers to test a lot of different things. We also used computers to see how a medicine called fluoxetine interacts with the MvfR/PqsR protein. Then we made some versions of fluoxetine that are similar but a little different to see if they can work better with the MvfR/PqsR protein. These derivatives were then checked using docking analysis and ADMET profiling. The assessment included how well they bind, their pharmacokinetics and safety details. Lab experiments were also done to confirm the results. These tests looked at the activity and biofilm inhibition of fluoxetine against Mvfr protein. Fluoxetine showed a binding affinity with the MvfR receptor at -8.4 kcal/mol. The antibacterial activity was confirmed through experiments. The minimum amount needed to inhibit growth was 0.5 mg/mL. A significant decrease in biofilm biomass was seen at $p = 0.005$. This shows a reduction in biofilm. Some derivatives showed binding interactions. They also had ADMET profiles compared to the original compound. The research suggests that fluoxetine could work as an antivirulence agent against Pseudomonas aeruginosa infections by targeting MvfR. The findings support using existing drugs for purposes as a good way to find antimicrobials. However more experiments and, in studies are needed to confirm the therapeutic importance. More work is required to understand the potential of fluoxetine and its derivatives. The results are promising, further research is necessary.

Highlights

- This research employed *in silico* techniques to repurpose fluoxetine. The study seeks to target MvfR in *Pseudomonas aeruginosa* because MvfR regulates virulence and is invloved in biofilm formation.
- Fluoxetine analogs were designed through bioisosteric substitution methods by changing the functional group of fluoxetine. The primary objective was to enhance adhesion strength. It sought to improve drug action within the body.
- The chosen analogs underwent testing through molecular docking and ADMET evaluation. Among the compounds, two exhibited negative interactions with P-

*Corresponding Author: mumtazzarkhaiz6@gmail.com

glycoprotein (P-gp) and the remaining two exhibited favorable P-gp interactions.

- Laboratory tests verified the antibacterial and anti-biofilm properties of fluoxetine and its derivatives against *P. aeruginosa*. These findings back their possibility of being repurposed (agents that combat microorganisms).
- By aiming virulence elements instead of bacterial viability, this study presented an alternate strategy to address biofilm-associated infections.

1. INTRODUCTION

Pseudomonas aeruginosa is a common opportunistic pathogen (takes advantage of a weak immune system to cause a disease) and can cause infections, especially if the immune system is compromised. It endures in various environments via multiple metabolic pathways and regulatory genes [1, 2]. These systems assist it in enduring tough conditions. This flexibility enables the bacteria to generate various virulence factors. It aids in building resistance strategies. Consequently, treating infections becomes challenging. This is especially severe in individuals with cystic fibrosis [3, 4]. Owing to its significance in clinical settings and notable resistance, *P. aeruginosa* is regarded as a key pathogen for investigation and medication advancement [5, 6]. The World Health Organization (WHO) categorizes it as a significant pathogen. This is due to its strong resistance and its links to higher rates of illness and mortality [7].

Biofilms are created by various bacteria, such as *P. aeruginosa*. These are organized groups of bacteria. They are encompassed by a protective layer they have generated themselves [8, 9]. The development of biofilm assists bacteria in enduring challenging circumstances. Such conditions consist of nutrient scarcity and exposure to antibiotics [10]. *P. aeruginosa* is recognized for creating robust biofilms. It is often associated with biofilm-related infections [11, 12]. Biofilm formation is controlled by quorum sensing (QS) systems. These systems allow bacteria to interact with each other. They additionally assist bacteria in detecting population density and environmental cues [13, 14]. In this manner, they control virulence, biofilm formation, and lasting survival [15].

1.1. Antimicrobial Resistance

Resistance to antimicrobials is a health problem around the world. It makes existing treatments less effective. This issue also puts a lot of pressure on healthcare systems [16]. *Pseudomonas aeruginosa* show resistance in ways. These include using efflux pumps to push out antibiotics having membrane permeability and using virulence pathways controlled by quorum sensing [17]. All these processes together lead to multidrug resistance. The overuse and misuse of antibiotics have made resistance worse. So we urgently need treatment strategies. The excessive use and improper application of antibiotics have exacerbated resistance creating a need, for treatments [18].

A promising approach is to focus on virulence regulators rather than directly eliminating bacteria. For this, an essential regulator is MvfR (PqsR) protein. It functions as a transcription factor involved in quorum sensing and regulates genes that influence virulence, biofilm development, as well as, bacterial survival in *P. aeruginosa* [19]. Despite extensive research on MvfR, there are still few effective drugs that specifically target it [20]. Conventional drug development takes a long time and it is not cost effective at all.

In numerous instances, it proves to be less effective against resistant bacteria [21].

In silico strategies, including molecular docking, virtual screening, and molecular dynamics (MD) simulations offers efficient alternatives for identifying potential inhibitors of critical bacterial targets such as MvfR [22]. Drug repurposing, in particular provides an attractive strategy by identifying new antimicrobial applications for approved drugs with known safety profiles [23]. This approach may accelerate translational potential while reducing development costs and the duration require to form a new drug [24].

1.2. Scope

In this study, the antibacterial and antibiofilm activity of fluoxetine against *Pseudomonas aeruginosa* was evaluated. The interaction with the MvfR regulator was studied using computational methods and potential drug candidates were identified against *P. aeruginosa*. The techniques included molecular docking and computational drug design [25, 26]. Wet-lab experiments were performed to test antibacterial activity and biofilm inhibition by fluoxetine. *In silico* methods were further applied to study fluoxetine binding to MvfR protein. These methods helped design improved derivatives with better activity. An integrated experimental and computational approach has not yet been fully applied to fluoxetine as an MvfR-targeting agent. This gap was addressed in the present study. Wet-lab validation was combined with *in silico* drug repurposing methods. Therefore, this combined approach helped explore new strategies to combat antimicrobial resistance.

2. MATERIALS AND METHODS

The research employed both laboratory experiments and computational techniques. It assessed the antimicrobial and anti-biofilm effects of fluoxetine. Additionally, this study examined fluoxetine which can be utilized as a repurpose inhibitor aimed at the MvfR regulator of *Pseudomonas aeruginosa*.

2.1. Preparation of Bacterial Cultures

A culture of *P. aeruginosa* was incubated overnight in nutrient broth at 37 °C with agitation. The culture was allowed to develop until the logarithmic phase was attained. The bacterial suspension was modified to 0.5 McFarland (1.5×10^8 CFU/mL) with sterile saline. This maintained uniformity across all following experiments.

2.2. Antibacterial Activity Assay

Standard bacterial suspensions were spread evenly on Mueller Hinton agar plates and wells bored under sterile conditions. Test samples were added into the wells. Eventually the plates were incubated at 37 °C for 24 hours. Following incubation, the zones of inhibition were assessed in millimeters. All experiments have been conducted in sets of three. (n = 3) [27]. The antibacterial activity results are presented in Figures 9a and 9b.

2.3. Minimum Inhibitory Concentration (MIC)

The Minimum Inhibitory Concentration was found by using a method where we diluted something many times. The Minimum Inhibitory Concentration is the amount that stops bacteria from growing. We did every experiment three times to make sure the results are correct [28].

2.4. Biofilm Inhibition Assay

A 96 well plate was used to check how well biofilms were suppressed. The

biofilms were left to grow for some time. Then cells that were not stuck were washed away. The biofilm that was left was stained with a dye called crystal violet. The purple dye was then removed using a liquid. This helped to get a reading of how much biofilm was present. The reading was taken at a light wavelength. If the reading was lower, than the control it meant the biofilm was inhibited. All the experiments were done three times to ensure accuracy [29]. The anti-biofilm activity results are presented in Figures 10a and 10b.

2.5. Target Protein Analysis

The MvfR protein, also known as PqsR was picked from databases that deal with virulence and resistance. We used bioinformatics tools to do this. These computer tools helped us get the sequence analyze the domain check the structure and find the binding pockets of the MvfR protein. We used the crystal structure, which's available, with the PDB ID: 6B8A, to see how well the MvfR protein and other things stick together. The extra information has the results of the validation and more analyses of the MvfR protein. Protein target validation, genomic annotation and virulence profiling and binding site prediction are presented in Figures 1, 2, and 3, respectively.

2.6. Ligand Identification and Optimisation

Fluoxetine was chosen as the ligand. It was selected because of its chemical makeup. How it works as a medicine. Information on its structure and how it is processed in the body was taken from chemical databases. Computer methods were used to study how ligands interact with proteins. These methods were also used to design versions of the ligand. The goal was to understand how Fluoxetine works and how it can be made better. Fluoxetines properties make it a good candidate, for this kind of study. The fluoxetine analogues generated during the optimisation process are summarized in Table 3, while their chemical structures are shown in Figures 8a–e.

2.6.1. ADMET Analysis. SwissADME, pkCSM, and ProTox 3.0 databases predicted ADMET properties which include absorption, distribution, metabolism, excretion, and toxicity [30–32]. The predicted ADMET profiles of fluoxetine and its analogues are presented in Table 4.

2.7. Molecular Docking

Chimera and PyRx with AutoDock Vina were used for protein preparation and docking. A grid box of 26 × 26 × 26 Å was set while centred at X = 24.8, Y = –22.7, and Z = 12.8 to target the multi virulence factor (MvfR) active site. Docking results were evaluated using binding affinity (kcal/mol). Fluoxetine derivates were filtered out on the basis of the best docking poses. The protein preparation and docking workflow is illustrated in Figures 4 and 5.

2.7.1. Post-docking Interaction Analysis. PLIP was used to analyse protein–ligand interactions and Discovery Studio to visualise the results. Key non-covalent interactions were identified. All these interactions contribute to binding stability. The 2D and 3D docked complexes are shown in Figures 6a and 6b, while the protein–ligand interaction profile is presented in Table 1.

2.8. Molecular Dynamics (MD) Simulation

iMODS was used to perform normal mode analysis. This was done to study the stability and flexibility of the fluoxetine–MvfR complex under physiological conditions [33]. The molecular dynamics

simulation results are shown in Figures 7a–f, whereas the binding free energy analysis is presented in Table 2.

2.9. Bioisosteric Replacement

Insilico tool (Xundrug) was used to design bioisosteric modifications. The goal was to improve binding affinity and selectivity. It aimed to enhance ADMET properties while reducing toxicity [34]. The chemical structures of the designed analogues are shown in Figures 8A–E, and the bioisosteric modifications introduced are summarized in Table 5.

3. RESULTS AND DISCUSSION

3.1. Protein Target Validation (MvfR)

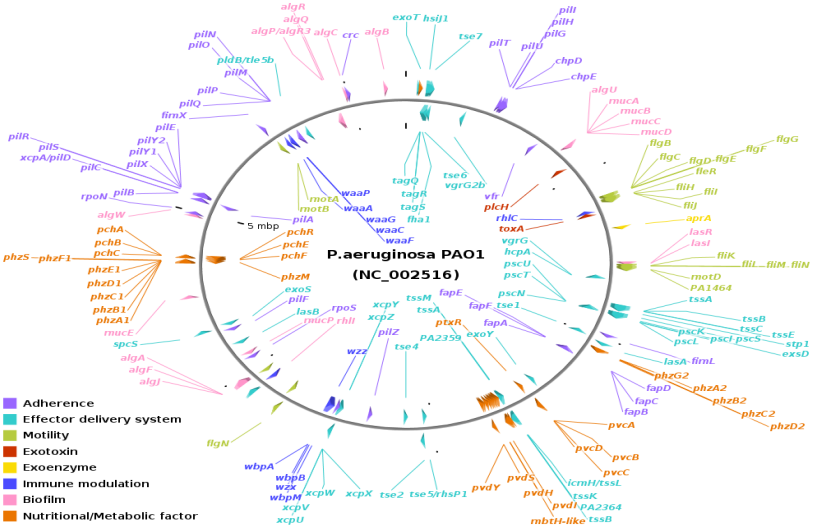

Figure 1. Identification of Virulence-associated Genes in ***P. aeruginosa*** using the Virulence Factor Database (VFDB)
Source: Virulence Factor Database (VFDB)

Several virulence-related genes were identified through VFDB analysis. These genes are involved in pathogenicity. They are also associated with quorum sensing and biofilm formation. From this examination, the quorum sensing regulator MvfR (PqsR) was chosen as the intended protein. It was selected for additional experimental and computational investigations. This is due to its critical function in regulating virulence in *Pseudomonas aeruginosa*. It is likewise crucial in the formation of biofilms. Earlier research has indicated that MvfR is engaged in the production of virulence factors and quorum sensing [35].

The PATRIC database analysis provides detailed genomic information and functional annotation of *P. aeruginosa*. This confirms the presence of multiple virulence-associated genes involved in pathogenicity and host infection. This analysis further supports the selection of *P. aeruginosa* as the study organism and highlights the relevance of targeting virulence regulatory proteins, such as MvfR in therapeutic investigations.

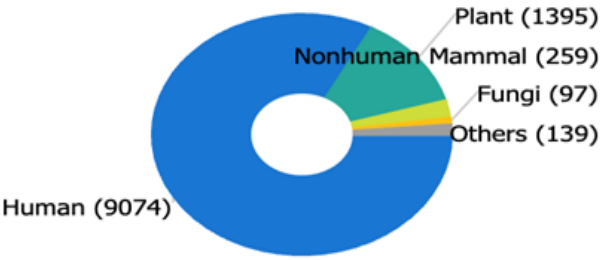

Figure 2. Genomic Annotation and Virulence Profiling of *Pseudomonas aeruginosa* using the Pathosystems Resource Integration Center (PATRIC) Database
Source: Pathosystems Resource Integration Center (PATRIC) database.

3.2. Structural and Functional Analysis of Proteins

A detailed computational characterization of the MvfR protein was performed, including the analysis of physicochemical properties (Section 3.2.1; ProtParam), prediction of secondary structure (Section 3.2.2; SOPMA), and subcellular localization (Section 3.2.3; WolfPSORT). In addition, protein–protein interaction analysis using STRING and hub gene identification (Section 3.2.4) were conducted to further explore the functional interaction network of MvfR. These analyses are provided in the Supplementary Data and collectively support the functional stability and biological relevance of MvfR as a regulatory protein involved in quorum sensing.

3.3. Protein 3d Structure Analysis and Characterization

A comprehensive structural validation of the MvfR protein was conducted, including three-dimensional structure visualization (Section 3.3.1 PDB), Ramachandran plot analysis, and ERRAT quality assessment. These structural evaluations, presented in the Supplementary Data confirmed the reliability and suitability of the MvfR protein structure for subsequent molecular docking and *in silico* studies.

3.4. Binding Site Prediction

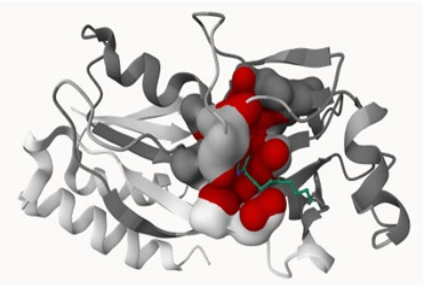

Figure 3. The Three-dimensional Structure of the MvfR Protein Illustrates Several Regions of Interest

In the visual representation, predicted binding sites are shown in red. Predicted active sites are also shown in red. These regions are important for molecular interactions. Ligand-binding sites are shown in green (regions where ligands are expected to bind).

3.5. Ligand Verification and Structural Analysis

Ligand validation and examination were carried out for fluoxetine, chloroquine, favipiravir, and levofloxacin. SMILES representation and 2D diagrams of all ligands are included in the Additional Information (supplementary data file).

3.6. Pharmacokinetics, Drug-Likeness, and Toxicity Prediction

The predicted results of pharmacokinetic and toxicity characteristics of fluoxetine were generated, suggesting favorable absorption and permeability, satisfactory drug-likeness and minimal toxicity . For instance, it falls in Class IV; the LD50 is 1190 mg/kg. Comprehensive SWISS ADME and ProTox-II prediction outcomes, including visual representations the results are included in the Supplementary Data file.

3.7. Protein Preparation and Docking Analysis Tools

Throughout this procedure, the native ligand and H_2O molecules were deleted. Hydrogen atoms were subsequently incorporated, and Gasteiger charges were allocated to make the protein structure ready for molecular docking.

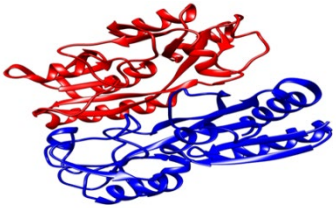

Figure 4. The MvfR Protein was Readied for Docking with Chimera

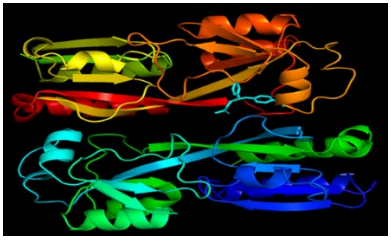

Figure 5. Levofloxacin was Used as Control Compound and Fluoxetine, Chloroquine and Favipiravir were Docked for Binding Affinity Study to MvfR protein.

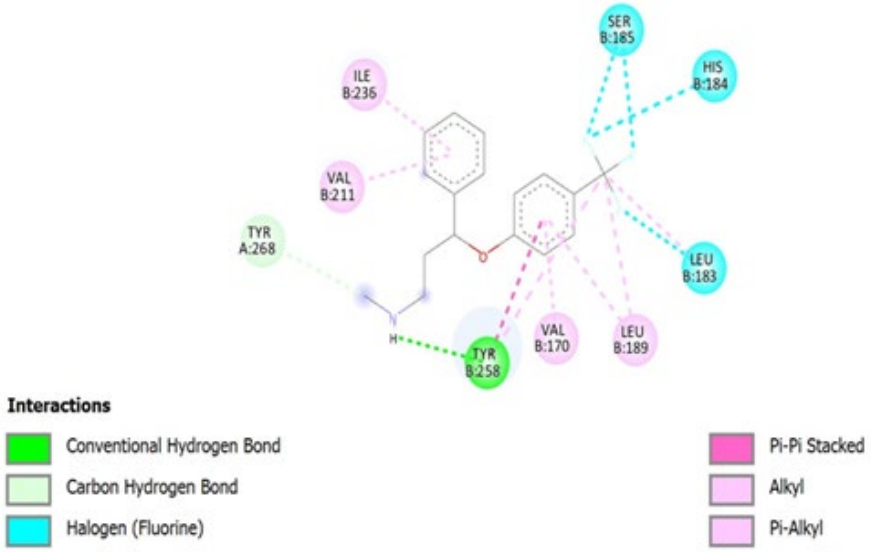

Figure 6a. Two-dimensional (2D) Docked View

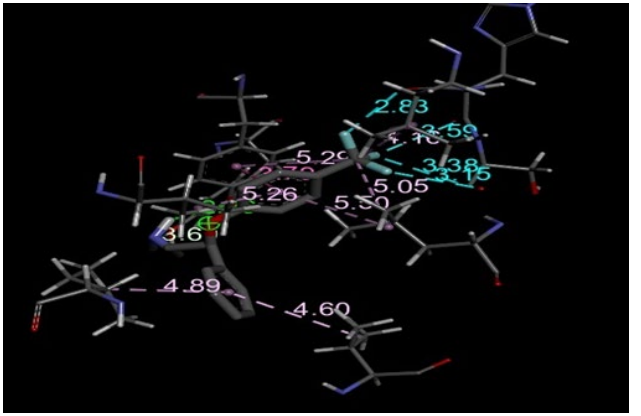

Figure 6b. Three-dimensional (3D) Docked View

Binding affinity of fluoxetine (-8.4 kcal/mol), levofloxacin (−8.0) kcal/mol, followed by Chloroquine (−6.8 kcal/mol) and Favipiravir (−5.4 kcal/mol) therefore, fluoxetine showed the lowest binding energy. These results show that fluoxetine exhibits a greater binding energy for MvfR than the other compounds tested indicating its potential as a hopeful treatment option for *Pseudomonas aeruginosa*. Interactions between protein and ligand were detected through PLIP and represented in both 2D and 3D formats using Discovery Studio Visualizer. Comparable computational methods, such as docking and molecular dynamics simulations have been utilized in past drug repurposing investigations aimed at MvfR to uncover possible inhibitors for *P. aeruginosa* [36, 37].

The 2D docked illustrate interactions between fluoxetine and the MvfR protein. It clearly displays connections and contact points. The 3D docked image presents a spatial view of the docking configuration that aids in comprehending how fluoxetine accommodates within the MvfR binding site.

Table 1. PLIP- Protein–Ligand Interactions Between Fluoxetine and MvfR

No.	Residue (Chain)	Interaction Type	Distance (Å)	
1	ILE186 (B)	Hydrophobic	3.38	
2	VAL211 (B)	Hydrophobic	3.78 / 3.67	Two separate contacts
3	TRP234 (B)	Hydrophobic	3.70 / 3.79	Two separate contacts
4	ILE236 (B)	Hydrophobic	3.68 / 3.59	Two separate contacts
5	TYR258 (B)	Hydrophobic	3.85 / 3.70	Also involved in H-bond and π-stacking
6	ILE263 (B)	Hydrophobic	3.86 / 3.99	Two separate contacts
7	TYR258 (B)	Hydrogen Bond	2.15	Donor: N3 (Ligand), Acceptor: O3 (Protein)
8	LYS266 (A)	Hydrogen Bond	3.26	Electrostatic: N3+ (Ligand) to N3 (Protein)
9	TYR258 (B)	π–π Stacking	3.79	Planar distance: 2.82 Å, Offset: 1.38 Å

The primary non-covalent interactions occurring between fluoxetine and the MvfR protein are outlined in Table 1. The interactions consist of hydrophobic interactions, hydrogen bonds, and π–π stacking engagements. The PLIP server identified and verified these interactions.

Multiple non-covalent interactions were detected in the fluoxetine–MvfR complex which suggests consistent attachment in the active site. Moreover, the majority of interactions were hydrophobic and the involved residues include ILE186, VAL211, TRP234, ILE236, TYR258, and ILE263. Interaction distances varied between 3.38 and 3.99 Å. Certain residues displayed multiple contact points as well as Polar interactions. Two hydrogen bonds formed between fluoxetine and residues: TYR258 and LYS266.

Their bond lengths were 2.15 Å and 3.26 Å. A π–π stacking interaction with residue TYR258 showed improved binding strength and specificity. Overall, these interactions supported strong and stable binding of fluoxetine in the MvfR pocket.

3.8. Molecular Dynamics (MD) Stimulation

Molecular dynamics (MD) simulations were performed using iMODS and Google Colab both. These simulations showed the stability and flexibility of the MvfR–fluoxetine complex. The results from iMODS (version 3.8.1) are provided in the Supplementary Data and google colab results are shown below.

The plot illustrates the interaction energy profile between fluoxetine and MvfR during the MD simulation, including total interaction energy (blue), electrostatic energy (green), and van der Waals energy (red). The mean total interaction energy was −37.20 ± 3.03 kcal/mol which indicated a stable ligand–protein interaction between the complex throughout the simulation. This showed that hydrophobic forces played the main role in stabilizing the complex. Van der Waals energy remained negative during the simulation whereas, electrostatic energy remained positive. This suggests a weak or slightly unfavorable contribution. A gradual decrease in total interaction energy showed that the complex became more stable over time.

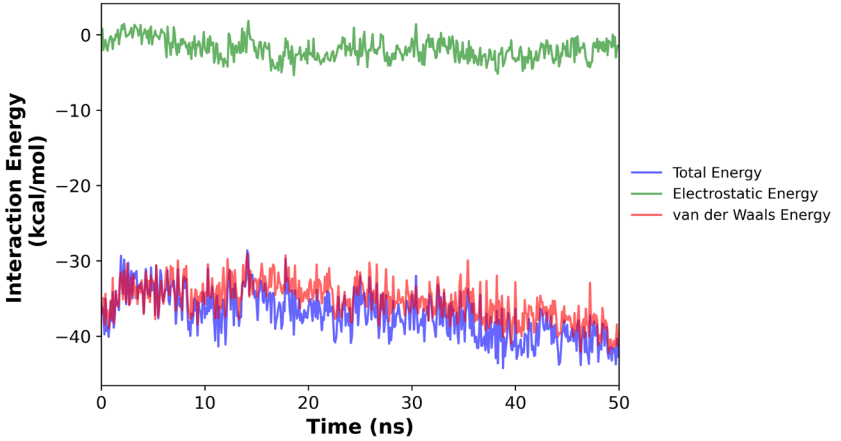

Figure 7a. Interaction Energy Analysis Over Time

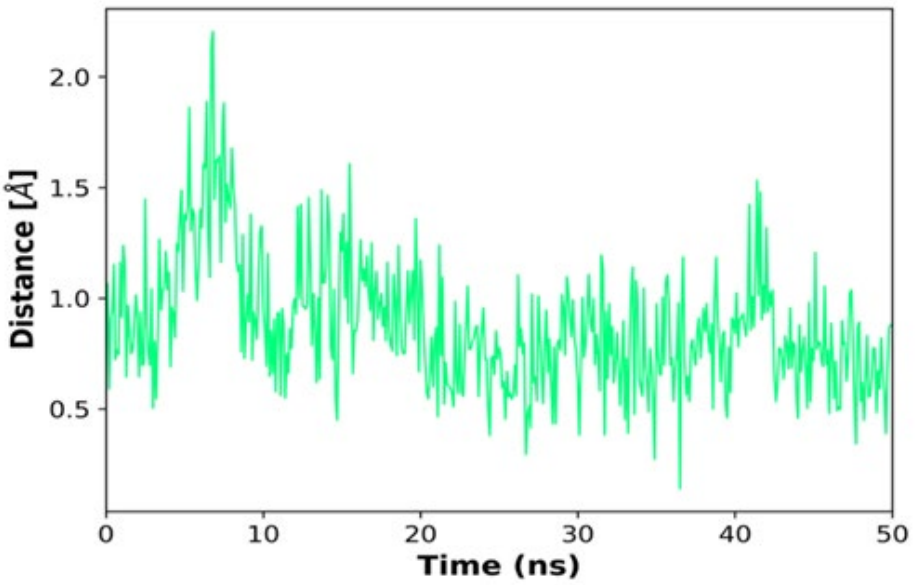

Figure 7b. Residue Contact Distance Over Time

The plot also shows the distance between selected binding-site residues and a reference point over 50 ns. The average distance was 0.88 ± 0.29 Å indicating strong and stable contact. Small fluctuations were observed in the first 10 ns. During this time, distances increased to about 2–3 Å. This likely occurred due to structural adjustment. After this phase, distances remained below 1 Å. This indicates stable interactions.

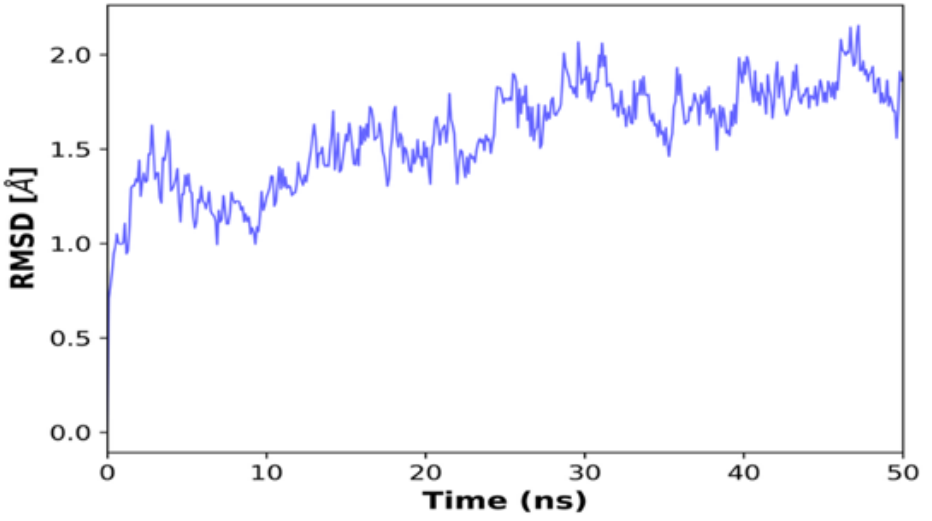

Figure 7c. Root Mean Square Deviation (RMSD) of the System

The RMSD graph shows an initial rise to about 1.5 Å in the first 10 ns. After 20 ns, it stabilized between 1.8 and 2.0 Å. Eventually, the complex reached a stable structure early and remained stable for the rest of the simulation.

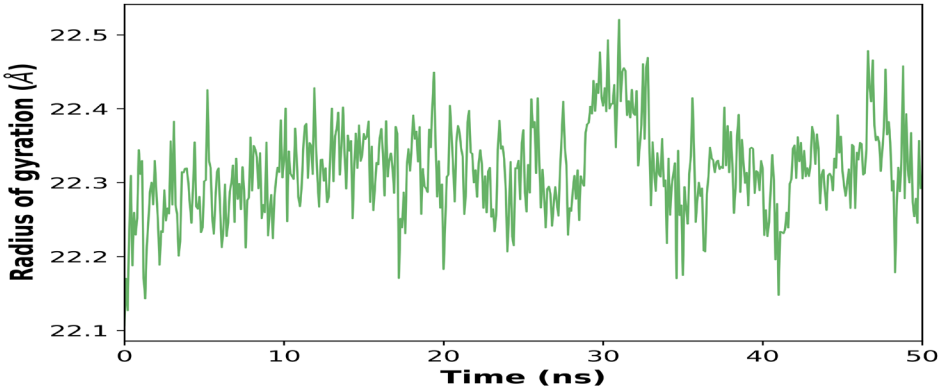

Figure 7d. Radius of Gyration Over Time

The radius of gyration was maintained between 22.1 and 22.5 Å during the 50 ns simulation. This demonstrated that the protein stayed compact because no major changes were observed. No folding or unfolding occurred thus, the structure remained stable.

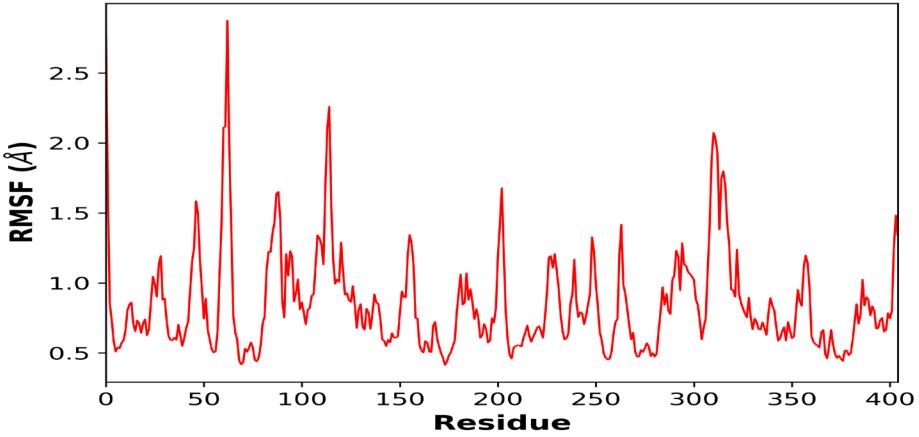

Figure 7e. RMSF (Root Mean Square Fluctuation)

RMSF analysis revealed that most residues exhibited fluctuations between 0.5 and 1.0 Å ,as well as, increased flexibility was observed around residues, approximately at positions 40, 90, 180, and 300 (where fluctuations reached up to 2.5 Å). This highlighted at the probably adaptable loop or surface areas. The central area of the protein stayed stable and firm.

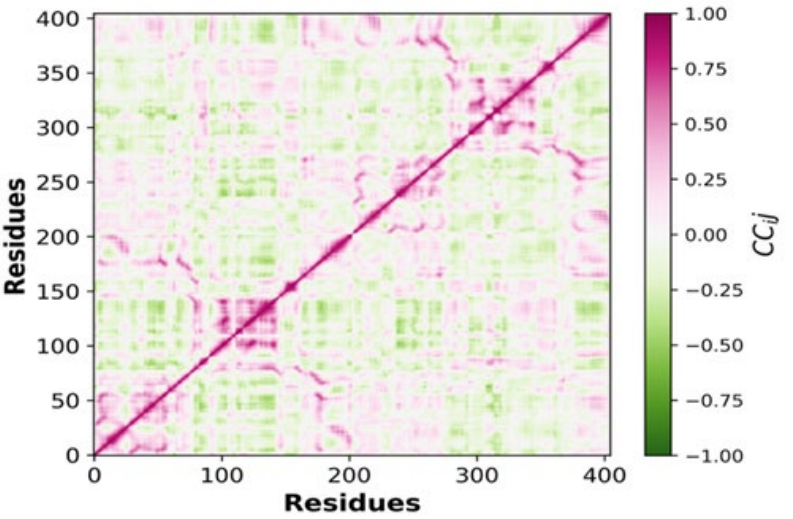

Figure 7f. Dynamic Cross-Correlation Matrix (DCCM)

DCCM analysis showed both correlated and anti-correlated residue motions thereby, indicating coordinated internal movements within the protein. Such collective dynamics may contribute to functional stability and ligand accommodation.

Table 2. MM-PBSA and MM-GBSA Binding Free Energy Analysis

Method	ΔG_{total} (kcal/mol)	Interaction Energy (kcal/mol)	Key Interpretation
MM-PBSA	+2.02 ± 3.49	–37.20 ± 3.03	Weak binding due to solvation penalty
MM-GBSA	–24.11 ± 2.00	–37.20 ± 3.03	Strong binding, reduced solvation penalty

MM-PBSA findings indicated a somewhat less favorable binding free energy (ΔG = +2.02 kcal/mol). This was primarily because of a considerable solvation penalty. Interactions in the gas phase remained beneficial. Conversely, MM-GBSA estimated a favorable binding free energy (ΔG ≈ −24.11 kcal/mol) illustrating a constraint of MM-PBSA, significantly influenced by solvation effects. MM-GBSA is thus regarded as more dependable and a reliable estimate for this system.

3.9. Ligand Design and Structural Optimization for MvfR Inhibition

Four main criteria were emphasized in ligand selection through bioisosteric replacement: i) synthetic accessibility, ii) clogP, iii) topological polar surface area (TPSA), and iv) Caco-2 permeability. Compounds with low synthetic accessibility ratings guaranteed practicality of synthesis, as well as Equilibrium lipophilicity (clogP ranging from 1 to 3), reduced TPSA, and lastly, elevated Caco-2.

Permeability was deemed crucial for sufficient solubility, membrane permeability and gut uptake. These parameters together informed the choice of ligands appropriate for ongoing advancement targeting *P. aeruginosa*.

Table 3. Analogs

	SMILES	Synthetic Accessibility	Energy Affinity (kcal/mol)	GI Absorption	BBB Penetration	Protox Class
Fluoxetine	CNCCC(C1=CC=CC=C1)OC2=CC=C(C=C2)C(F)(F)F	2.56	-8.4	High	Yes	3
Analog 1	CNCC(Oc1ccc(C(F)(F)F)cc1)c1cccc2ccccc12	2.581	-9.4	High	No	4
Analog 2	CNC(=O)CC(Oc1ccc(C(F)(F)F)cc1)c1ccccc1	2.6	-8.9	High	Yes	3
Analog 3	CNCCC(Oc1ccc(-c2ccccc2)cc1)c1ccccc1	2.78	-9.2	High	Yes	3
Analog 4	FC(F)(F)c1ccc(OC(c2ccccc2)C2CCNCC2)cc1	2.78	-8.8	High	Yes	3
Analog 5	CNc1cc(Oc2ccc(C(F)(F)F)cc2)cc(-c2ccccc2)c1	2.61	-9.6	Low	No	4
Analog 6	CN1C2CCC1CC(OC(c1ccccc1)c1ccc(C(F)(F)F)cc1)C2	4.59	-9.5	Low	No	3

The analogs were generated utilizing a bioisosteric substitution tool. Functional groups of fluoxetine were changed throughout this process in order to generate derivatives. Moreover, fluoxetine analogues 2, 3, and 4 demonstrated favorable gastrointestinal uptake and blood–brain barrier (BBB) permeability. In comparison, Analogue 1 demonstrated strong gastrointestinal uptake but no BBB infiltration. After filtration, four analogs were chosen for additional assessment. On the other hand, other compounds were eliminated because of inadequate absorption and minimal BBB permeability. Toxicity assessment with ProTox-II indicated that three compounds belong to class 3 (moderate toxicity). One example was Class 4 (low toxicity). The findings suggested that these substances could be appropriate for additional examination.

3.9.1. ADMET Analysis.

This section provides an assessment of the ADMET characteristics of fluoxetine and its formulated substitutes. Emphasis is directed towards physicochemical, pharmacokinetic, and medicinal chemistry attributes. Multiple parameters were examined, such as molecular weight, TPSA, and rotatable bonds, solubility in water (Log S), fat affinity (Log P), absorption in the gastrointestinal tract, blood-brain barrier permeability, P-glycoprotein (P-gp) interaction, CYP enzyme inhibition, and drug resemblance parameters like Lipinski's Rule of Five, bioavailability, ease of synthesis, and PAINS/Brenk notifications.

3.9.1.1. Physicochemical Characteristics. Molecular weights were determined to vary between 309.33 and

345.36 g/mol, along with comparable TPSA values were seen across all compounds. The existence of five to seven movable bonds further suggested favorable membrane permeability. Additionally, Log S values indicated moderate to low solubility in water.

3.9.1.2. Pharmacokinetics. High gastrointestinal absorption was predicted for all compounds indicating suitability for oral administration. BBB permeability prediction for fluoxetine and Analogs 2–4, while Analogs 1 and 4 were not expected to cross the BBB. CYP1A2 inhibition was predicted for fluoxetine and Analog 2 ,however Analogs 1 and 4 were identified as non-inhibitors, showing differences in metabolic behaviour.

3.9.1.3. Drug-likeness and Medicinal Chemistry. Synthetic accessibility scores (2.56–2.78) suggested a moderate level of ease in synthesis. The majority of compounds adhered to Lipinski's Rule of Five, though slight infringements were noted in Analogs 1 and 3 (MLOGP > 4.15) which means high lipophilicity. All substances demonstrated satisfactory bioavailability ratings (0.55). No PAINS or Brenk alerts were found, emphasising positive drug-likeness profiles.

3.9.2. Chemical Structures of Fluoxetine along with its Analog. The design of fluoxetine analogs aimed to enhance ligand–target interactions and improve predicted antibiofilm activity. Modifications mainly introduced in the aromatic ring, halogen positions, and amine groups. Each analog was filtered based on docking scores, binding affinity, and ADMET properties. For this study, only the most promising candidates were retained for further analysis done using insilico techniques.

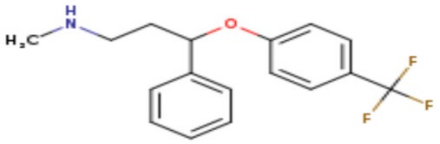

Figure 8a. Fluoxetine (-8.4 kcal/mol)

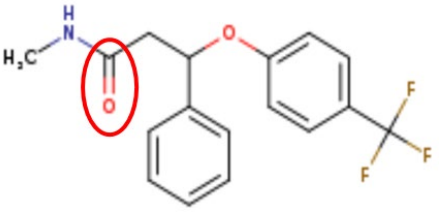

Figure 8b. -8.9 kcal/mol

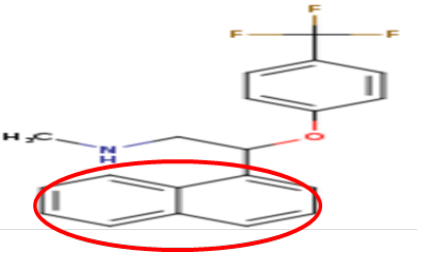

Figure 8c. -9.4 cal/mol

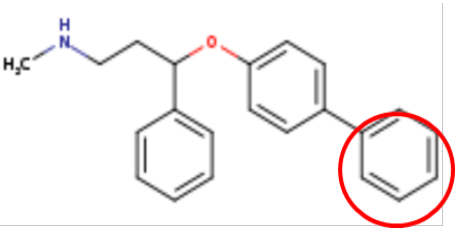

Figure 8d. -9.2 kcal/mol

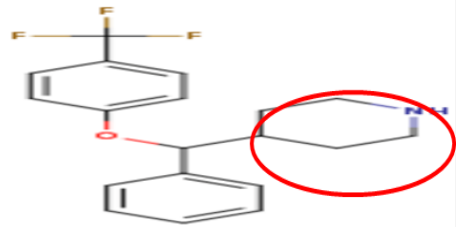

Figure 8e. -8.8 kcal/mol

Figure 8 (a–e) shows the 2D chemical structures of fluoxetine and its designed analogs and their binding energies are also

presented. The analogs were generated using bioisosteric substitution tool and thereby the derivatives showed improved binding affinity and drug-like properties.

Table 4. ADMET Analysis of Fluoxetine and its Analogs

Property	Fluoxetine	Analog 1 (-9.4)	Analog 2 (-8.9)	Analog 3 (-9.2)	Analog 4 (-8.8)
Molecular Weight (g/mol)	309.33	345.36	323.31	317.42	335.36
TPSA (Å²)	21.26	21.26	38.33	21.26	21.26
Num. Rotatable Bonds	7	6	7	7	5
Log S (ESOL)	-4.36	-5.29	-4.01	-5.04	-4.87
Solubility Class	Moderately soluble	Poorly Soluble	Moderately soluble	Moderately soluble	Moderately soluble
GI Absorption	High	High	High	High	High
BBB Permeant	Yes	No	Yes	Yes	Yes
P-gp Substrate	No	No	No	Yes	Yes
CYP1A2 Inhibitor	Yes	No	Yes	Yes	No
CYP2C9 Inhibitor	No	No	No	No	No
Consensus Log Po/w	4.32	4.92	3.7	4.59	4.46
Lipinski Rule	Yes; 0 violation	Yes; 1 violation: MLOGP>4.15	Yes; 0 violation	Yes; 1 violation: MLOGP>4.15	Yes; 0 violation
Bioavailability Score	0.55	0.55	0.55	0.55	0.55
Synthetic Accessibility	2.56	2.7	2.6	2.78	2.78
PAINS Alert	0 alert	0 alert	0 alert	0 alert	0 alert
Brenk Alert	0 alert	0 alert	0 alert	0 alert	0 alert

Table 5. The Bioisosteric Changes Introduced into the Fluoxetine Structure

Original Group	Replacement Group
-CH2-O- linkage in fluoxetine	ketone group (-C=O)
Fluorine atoms on the benzene ring	phenyl group (benzene ring)
Benzene ring	fused aromatic ring structure (biphenyl or similar)
N-methyl acetamide group	Secondary amine (R_2NH)

3.10. Antibacterial and Anti-Biofilm Activity of Fluoxetine and its Derivatives

Wet-lab experiments were conducted to confirm the computational predictions for antibacterial effectiveness and activity against biofilms. MIC assays demonstrated that fluoxetine suppressed the increase of *Pseudomonas aeruginosa*. Biofilm inhibition tests similarly indicated diminished biofilm biomass in relation to untreated controls suggesting possible interference with the development of biofilms.

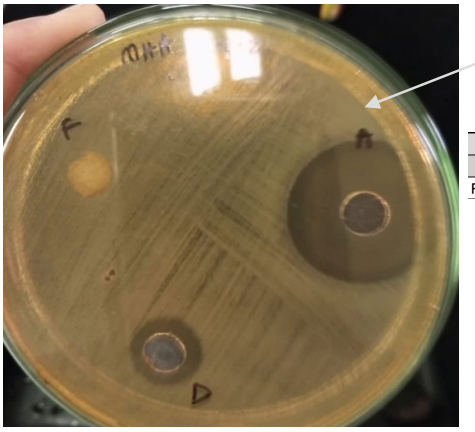

Fluoxetine against *P. aeuruginosa*

Samples	P. aeruginosa	
	Zone of inibition (mm)	MIC (%)
Fluoxetine	39	6.25

Figure 9 a,b. Fluoxetine against *P. aeuruginosa*

Fluoxetine showed clear antibacterial activity against *P. aeruginosa*. At 4 mg/mL, inhibition zones up to 39 mm were observed. The MIC was 0.5 mg/mL, where an inhibition zone of about 20 mm was recorded. These results show a concentration-dependent effect as strong inhibition was observed at higher concentrations. Some activity was also seen at lower concentrations, suggesting possible antibacterial potential that needs further study.

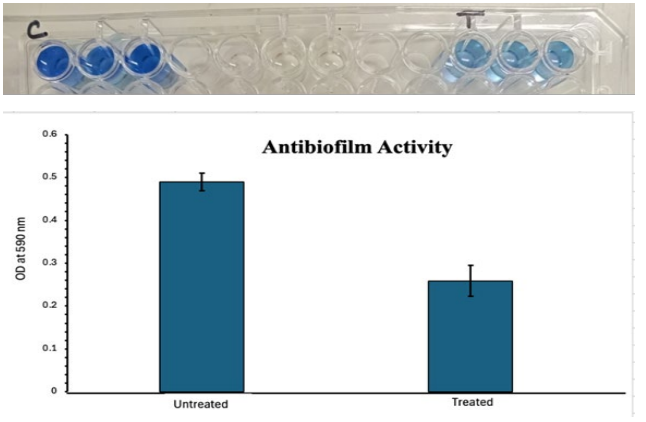

Figure 10 a,b. Anti-biofilm Activity

The antibiofilm activity of fluoxetine was evaluated using a crystal violet microtiter plate assay. Untreated wells showed a mean OD of 0.489 ± 0.02 at 590 nm demonstrating strong biofilm formation. In comparision with the treated samples showed a reduced OD of 0.346 ± 0.02. This reduction was statistically significant ($p = 0.005$). The results indicate that fluoxetine reduces biofilm formation in *P. aeruginosa* highlighting the activity of antidepressant drug against biofilm growth under the tested conditions. Previous studies have also shown that targeting quorum sensing regulators such as MvfR can reduce biofilm formation and virulence in *P. aeruginosa* [38, 39].

3.11. Conclusion

Fluoxetine was tested as a potential inhibitor of the MvfR (PqsR) quorum-sensing regulator in *P. aeruginosa*. Both *in silico* and wet-lab methods were used. Molecular docking showed good binding affinity (−8.4 kcal/mol). Bioisosteric optimization produced analogs with improved predicted pharmacokinetic properties. In vitro tests confirmed antibacterial and antibiofilm activity of fluoxetine. Overall, the results suggest that fluoxetine and its derivatives may affect MvfR-mediated virulence. However, further in vivo and mechanistic studies are required to confirm therapeutic potential.

Author Contribution

Affhan Shoaib: conceptualization, supervision, writing – review & editing. **Mumtaz Zarkhaiz:** data curation, methodology, writing – original draft.

Conflict of Interest

The authors of the manuscript have no financial or non-financial conflict of interest in the subject matter or materials discussed in this manuscript.

Data Availability Statement

Data supporting the findings of this study will be made available by the corresponding author upon request.

Funding Details

This work was supported by the institutional funds provided to the corresponding author.

Generative AI Disclosure Statement

The authors acknowledge the use of generative AI tools (e.g., ChatGPT) solely for language editing and improvement of the manuscript's readability. No AI tools were used in data collection, analysis, interpretation, or in drawing scientific conclusions. All core research work and intellectual content were produced entirely by the authors.

REFERENCES

1. Lyu J, Chen H, Bao J, et al. Clinical distribution and drug resistance of *Pseudomonas aeruginosa* in Guangzhou, China from 2017 to 2021. *J Clin Med.* 2023;12(3):e1189. https://doi.org/10.3390/jcm12031189
2. Chen YT, Yang KX, Dai ZY, et al. Repressed central carbon metabolism and its effect on related metabolic pathways in cefoperazone/sulbactam-resistant *Pseudomonas aeruginosa*. *Front Microbiol.* 2022;13:e847634. https://doi.org/10.3389/fmicb.2022.847634
3. Mukherjee S, Bassler BL. Bacterial quorum sensing in complex and dynamically changing environments. *Nat Rev Microbiol.* 2019;17(6):371-382. https://doi.org/10.1038/s41579-019-0186-5
4. Al-Wrafy F, Brzozowska E, Górska S, Gamian A. Pathogenic factors of *Pseudomonas aeruginosa*—the role of biofilm in pathogenicity and as a target for phage therapy. *Adv Hyg Exp Med.*

2017;71:78-91. https://doi.org/10.5604/01.3001.0010.3792

5. Elfadadny A, Ragab RF, AlHarbi M, et al. Antimicrobial resistance of *Pseudomonas aeruginosa*: navigating clinical impacts, current resistance trends, and innovations in breaking therapies. *Front Microbiol.* 2024;15:e1374466. https://doi.org/10.3389/fmicb.2024.1374466
6. Li XY, Liu XG, Dong ZL, et al. The distribution, drug susceptibility, and dynamic trends of *Pseudomonas aeruginosa* infection in a tertiary hospital in China during 2016–2022. *Infect Drug Resist.* 2023;16:3525-3533. https://doi.org/10.2147/IDR.S408956
7. Pang Z, Raudonis R, Glick BR, Lin TJ, Cheng Z. Antibiotic resistance in *Pseudomonas aeruginosa*: mechanisms and alternative therapeutic strategies. *Biotechnol Adv.* 2019;37(1):177-192. https://doi.org/10.1016/j.biotechadv.2018.11.013
8. Donlan RM. Biofilms: microbial life on surfaces. *Emerg Infect Dis.* 2002;8(9):881-890. https://doi.org/10.3201/eid0809.020063
9. Kunwar A, Shrestha P, Shrestha S, Thapa S, Shrestha S, Amatya NM. Detection of biofilm formation among *Pseudomonas aeruginosa* isolated from burn patients. *Burns Open.* 2021;5(3):125-129. https://doi.org/10.1016/j.burnso.2021.04.001
10. Rollet C, Gal L, Guzzo J. Biofilm-detached cells, a transition from a sessile to a planktonic phenotype: a comparative study of adhesion and physiological characteristics in *Pseudomonas aeruginosa*. *FEMS Microbiol Lett.* 2009;290(2):135-142. https://doi.org/10.1111/j.1574-6968.2008.01423.x
11. Crespo A, Blanco-Cabra N, Torrents E. Aerobic vitamin B12 biosynthesis is essential for *Pseudomonas aeruginosa* class II ribonucleotide reductase activity during planktonic and biofilm growth. *Front Microbiol.* 2018;9:e986. https://doi.org/10.3389/fmicb.2018.00986
12. Ghafoor A, Hay ID, Rehm BHA. Role of exopolysaccharides in *Pseudomonas aeruginosa* biofilm formation and architecture. *Appl Environ Microbiol.* 2011;77(15):5238-5246. https://doi.org/10.1128/AEM.00637-11
13. Coughlan LM, Cotter PD, Hill C, Alvarez-Ordóñez A. New weapons to fight old enemies: novel strategies for the (bio)control of bacterial biofilms in the food industry. *Front Microbiol.* 2016;7:e1641. https://doi.org/10.3389/fmicb.2016.01641
14. Yan S, Wu G. Can biofilm be reversed through quorum sensing in *Pseudomonas aeruginosa*? *Front Microbiol.* 2019;10:e1582. https://doi.org/10.3389/fmicb.2019.01582
15. Mukherjee S, Jemielita M, Stergioula V, Tikhonov M, Bassler BL. Photosensing and quorum sensing are integrated to control *Pseudomonas aeruginosa* collective behaviors. *PLoS Biol.* 2019;17(12):e3000579. https://doi.org/10.1371/journal.pbio.3000579
16. Ramatla T, Nkhebenyane J, Lekota KE, et al. Global prevalence and antibiotic resistance profiles of carbapenem-resistant *Pseudomonas aeruginosa* reported from 2014 to 2024: a systematic review and meta-analysis. *Front Microbiol.*

2025;16:e1599070.

17. D'Costa VM, King CE, Kalan L, et al. Antibiotic resistance is ancient. *Nature.* 2011;477(7365):457-461. https://doi.org/10.1038/nature10388
18. Gaze WH, Krone SM, Larsson DGJ, et al. Influence of humans on evolution and mobilization of environmental antibiotic resistome. *Emerg Infect Dis.* 2013;19(7):e120871. https://doi.org/10.3201/eid1907.120871
19. Vieira TF, Magalhães RP, Cerqueira NM, Simões M, Sousa SF. Targeting *Pseudomonas aeruginosa* MvfR in the battle against biofilm formation: a multi-level computational approach. *Mol Syst Des Eng.* 2022;7(10):1294-1306. https://doi.org/10.1039/D2ME00088A
20. Allegretta G, Maurer CK, Eberhard J, et al. In-depth profiling of MvfR-regulated small molecules in *Pseudomonas aeruginosa* after quorum sensing inhibitor treatment. *Front Microbiol.* 2017;8:e924. https://doi.org/10.3389/fmicb.2017.00924
21. Li H, Maimaitiming M, Zhou Y, et al. Discovery of marine natural products as promising antibiotics against *Pseudomonas aeruginosa*. *Mar Drugs.* 2022;20(3):e192. https://doi.org/10.3390/md20030192
22. Sadiq S, Rana NF, Zahid MA, et al. Virtual screening of FDA-approved drugs against LasR of *Pseudomonas aeruginosa* for antibiofilm potential. *Molecules.* 2020;25(16):e3723. https://doi.org/10.3390/molecules25163723
23. Yang J, Guo K, Ren X, et al. Integrative multi-omics approach for drug repositioning in Alzheimer disease. *Precis Med.* 2025:e100050. https://doi.org/10.1016/j.prmedi.2025.100050
24. Barbarossa A, Rosato A, Corbo F, et al. Non-antibiotic drug repositioning as an alternative antimicrobial approach. *Antibiotics.* 2022;11(6):e816. https://doi.org/10.3390/antibiotics11060816
25. Jayaraman P, Sakharkar MK, Lim CS, Tang TH, Sakharkar KR. Activity and interactions of antibiotic and phytochemical combinations against *Pseudomonas aeruginosa* in vitro. *Int J Biol Sci.* 2010;6(6):556-568. https://doi.org/10.7150/ijbs.6.556
26. Das IJ, Bhatta K, Sarangi I, Samal HB. Innovative computational approaches in drug discovery and design. In: *Adv Pharmacol.* Elsevier; 2025:1-22. https://doi.org/10.1016/bs.apha.2025.01.006
27. Khan MA, Masood A, Ali K, Farid N, Bashir A, Dar MS. Green synthesis of silver, starch, and zinc oxide mediated nanoparticles with probiotics and plant extracts, their characterization and antibacterial activity. *Microb Pathog.* 2024;196:e107012. https://doi.org/10.1016/j.micpath.2024.107012
28. Karkuzhali K, Manivannan N, Venkatesan S. Antimicrobial activity of crude metabolites of *Vitis vinifera* using methanol extract against clinical pathogens. *J Pharm Bioallied Sci.* 2024;16(Suppl 2):S1186-S1190. https://doi.org/10.4103/jpbs.jpbs_521_23
29. Chadha J, Mudgil U, Khullar L, Ahuja P, Harjai K. Revitalizing common drugs for antibacterial, quorum quenching, and antivirulence potential against *Pseudomonas aeruginosa*: in vitro and *in silico* insights. *3 Biotech.* 2024;14(10):e219. https://doi.org/10.1007/s13205-024-04070-y

30. Daina A, Michielin O, Zoete V. SwissADME: a free web tool to evaluate pharmacokinetics, drug-likeness and medicinal chemistry friendliness of small molecules. *Sci Rep.* 2017;7:e42717. https://doi.org/10.1038/srep42717

31. Pires DE, Blundell TL, Ascher DB. pkCSM: predicting small-molecule pharmacokinetic and toxicity properties using graph-based signatures. *J Med Chem.* 2015;58(9):4066-4072. https://doi.org/10.1021/acs.jmedchem.5b00104

32. Banerjee P, Kemmler E, Dunkel M, Preissner R. ProTox 3.0: a webserver for the prediction of toxicity of chemicals. *Nucleic Acids Res.* 2024;52(W1):W513-W520. https://doi.org/10.1093/nar/gkae303

33. LeMoyne R, Mastroianni T, Whiting D, Tomycz N. Application of deep learning to distinguish multiple deep brain stimulation parameter configurations for the treatment of Parkinson disease. In: *IEEE.* 2020:1106-1111. https://doi.org/10.1109/ICMLA51294.2020.00178

34. Dick A, Cocklin S. Bioisosteric replacement as a tool in anti-HIV drug design. *Pharmaceuticals.* 2020;13(3):e36. https://doi.org/10.3390/ph13030036

35. Wheeler KM, Oh MW, Fusco J, et al. MvfR shapes *Pseudomonas aeruginosa* interactions in polymicrobial contexts: implications for targeted quorum-sensing inhibition. *Cells.* 2025;14(10):e744. https://doi.org/10.3390/cells14100744

36. Vieira TF, Magalhães RP, Simões M, Sousa SF. Drug repurposing targeting *Pseudomonas aeruginosa* MvfR using docking, virtual screening, molecular dynamics, and free-energy calculations. *Antibiotics.* 2022;11(2):e185. https://doi.org/10.3390/antibiotics11020185

37. Almihyawi RA, Al-Hasani HM, Jassim TS, Muhseen ZT, Zhang S, Chen G. Molecular insights into binding mode and interactions of structure-based virtually screened inhibitors for *Pseudomonas aeruginosa* MvfR. *Molecules.* 2021;26(22):e6811. https://doi.org/10.3390/molecules26226811

38. Schütz C, Ho DK, Hamed MM, et al. A new PqsR inverse agonist potentiates tobramycin efficacy to eradicate *Pseudomonas aeruginosa* biofilms. *Adv Sci.* 2021;8(12):e2004369. https://doi.org/10.1002/advs.202004369

39. Maura D, Rahme LG. Pharmacological inhibition of the *Pseudomonas aeruginosa* MvfR quorum-sensing system interferes with biofilm formation and potentiates antibiotic-mediated biofilm disruption. *Antimicrob Agents Chemother.* 2017;61(12):e01362-17. https://doi.org/10.1128/AAC.01362-17